Fifteenth International Symposium on Air Breathing Engines,
Bangalore, India September 2–7, 2001

DEVELOPMENT OF AN ADVANCED HIGH PRESSURE RATIO TRANSONIC FAN STAGE. PART-I: DESIGN AND ANALYSIS.

M.Z. Chen[+], Xu Liping[+], M.V.A.Murthy[++], M.Jayaraman[++], B.R.Pai[++], R.Prathapanayaka [++]

+ Beijing University of Aeronautics and Astronautics(BUAA), Beijing, P.R. China
++ Propulsion Division, National Aerospace Laboratories(NAL), Bangalore, India

Abstract

A high performance fan stage of pressure ratio 2.0 is being designed and developed under a joint programme between Chinese Aeronautical Establishment (CAE) China and National Aerospace Laboratories (NAL), Bangalore, India.. Special features of the aerodynamic design are i) forward blade sweep and lean to increase the ability to bear intake distortion ii) reverse camber fan tip to reduce losses via pre compression iii) low aspect ratio of the blades to maximize stall margin. The blade will be fabricated using laminates of Carbon/Epoxy composites with tip shroud so as to limit the blade stress and deformation. Stress analysis was carried out using MSC/NASTRAN Finite Element Package. The fan stage has undergone a series of design improvements. Comparison of typical results obtained at NAL and BUAA is shown for the final version of the fan stage TTT98-29.

Introduction

It is known that in a transonic fan rotor, a forward swept blading is an effective measure mainly for increasing the ability to bear distortion of flow entering the intake. With the availability of 3D flow codes the blade sweep could be optimized for improved efficiency and stall margin. The advantages associated with the forward sweep still need to be investigated to gain better understanding of the flow within the forward swept transonic rotor fan.

Effect of aerodynamic sweep was studied by A.R.Wadia[1] in GE Aircraft Engines(1997). It was concluded that the forward swept Rotor9 demonstrated a significant improvement in stall margin relative to already satisfactory level achieved by the unswept rotor. Aerodynamic design of NAL-CAE fan stage was mainly carried out at BUAA. The configuration Rotor 9[1] was studied during the design process. 3D analysis was carried out at both BUAA and NAL for comparative study.

Forward sweep in the blade is also associated with high local stresses in the blade. This needs detailed study of both aerodynamic design and stress analysis and choice of special blade material to withstand stresses. Detailed stress analysis was carried out at NAL.

Main design specification and features of the fan

Following were the design specification agreed for investigation.

Fan pressure ratio : 2.0
Tip diameter : 0.4m
Mass flow rate : 19.85 kg/sec
Diameter ratio : 0.45
Rotor tip speed : 470 m/sec

As the design proceeded, the rotor speed of 470m/sec was found to be sufficient.

It is difficult to achieve high level of forward sweep by the use of conventional metal blades, because of high stresses and weaker structural stability of the forward swept blades. To overcome this, it is necessary to employ Carbon Fiber Composite (CFC) together with a radical rotor structure design of integral blade, disc and tip shroud. The design with integral blade disc and tip shroud is aimed at flutter free transonic fan rotor.

Aerodynamic design and performance analysis

The aero thermodynamic design of the fan stage and the 3D flow analysis was carried at BUAA[2,3,4,5]. The final configuration of the fan stage was also analysed at NAL for comparision.

Computer codes and design procedure

Computer codes used at BUAA during the design included

- Meridional flow field design code (Wennerstrom);
- Blading code with arbitrary profile meanline (Wennerstrom);
- A/A* checking code (Developed at BUAA);
- 3D multistage viscous flow analysis code (Denton);
- Pre- and post processing codes for 3D computation (Developed at BUAA)

Computer codes used at NAL for 3D viscous flow analysis included

- 3D multistage RANS flow code with k-ε turbulence model 'un_B3d_ke' (W.N.Dawes)
- Pre- and post processing codes for 3D computation (Developed at NAL)

The steps of design procedure were setout as follows:

ST1. Meridional flow field design:

Basic aerodynamic properties and fan configurations were primarily determined at this stage with the help of empirical correlation and common wisdom. It follows the traditional design procedure.

ST2. Blading : This includes two sub-steps:

- Forming airfoils along stream surfaces, the camber lines of which are defined by flow angles along the stream surfaces and distributions of incidences and deviations.
- Stacking so obtained airfoils by a specified stacking line.

ST3. Checking A/A*:

Where A* stands for the critical area referred to the inlet flow condition of the stream tube. A is the real minimum area of the stream tube. Common practice requires this value to be greater than 1.02 – 1.03 for every stream tube, in order to safeguard a required through flow capacity.

ST4. Generating grid for 3D flow field calculation based on defined geometries of flow path and blades.

ST5. Calculation of 3D flow field for both design and off-design operations to check the flow field and correct the design. The matters we are concerned include

sign of flow separation anywhere in the passage;
selection of the incidences and deviations of the rotor and the stator;
the match of the stage;
the management of the passage shock wave system;
rotating stall/surge margin.

The above steps along with strength, vibration and flutter analysis are an iterative process. If any of these analyses show some unacceptable results, steps have to be repeated from ST1 or ST2 with necessary modifications.

Results of design and performance analysis

Meridional stream surface flow field design

Flow path design and main calculation results:

For specified pressure ratio and hub-tip radius ratio, the configuration of flow path is mainly determined by the options of outer and inner contours, aspect ratios of rotor and stator, the area contraction ratio from inlet to outlet.

The design pressure ratio is chosen to be 5% higher than specification value 2.0 to ensure required surge margin.

The air angle at exit of stator is set to be zero.

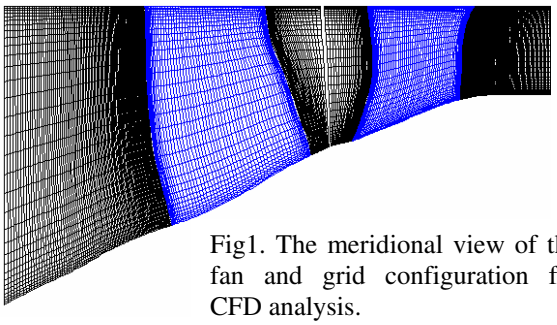

Fig1. The meridional view of the fan and grid configuration for CFD analysis.

Fig1. Shows the meridional view of the fan. The outer radius of the stage is kept constant for simplicity. However the rotor hub is carefully contoured in order to achieve better local velocity control, especially to avoid hub corner separation, which was present in some earlier designs.

The inner contour of stator section is a smooth curve connecting the inlet and outlet of stator. The aspect ratios of rotor and stator are in the range close to 1.0.

The value of area contraction is so chosen that at mid span the axial velocity ratio C_{2a}/C_{1a} ~ 0.8 for rotor, and ~ 1.2 for stator, in compliance with the common design practice.

The number of rotor blades is 17, that of stator blades is 30.

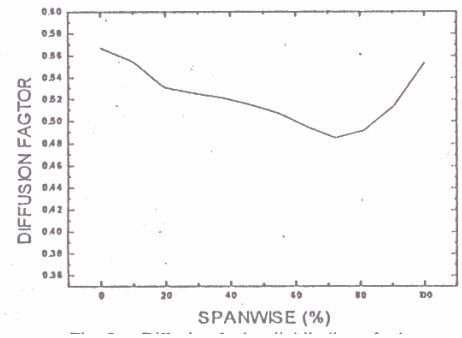

Fig 2a: Diffusion factor distribution of rotor.

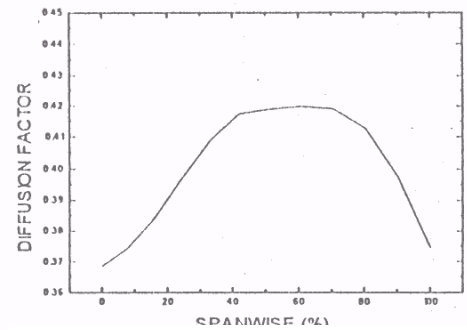

Fig 2b: Diffusion factor distribution of stator

The diffusion factor distributions are shown on fig2.a and fig2.b for rotor and stator, respectively. It should be noted that after careful tuning, the diffusion factor is contained within the acceptable limit, although the loading level is quite high.

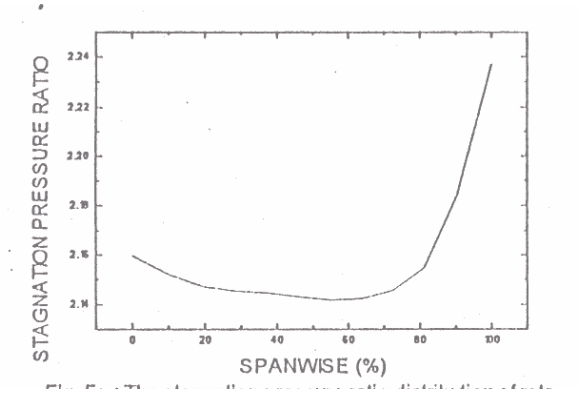

Fig 3a: The stagnation pressure ratio distribution of rotor

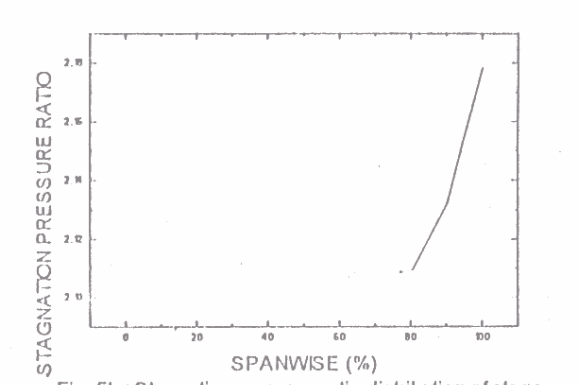

Fig 3b: Stagnation pressure ratio distribution of stage

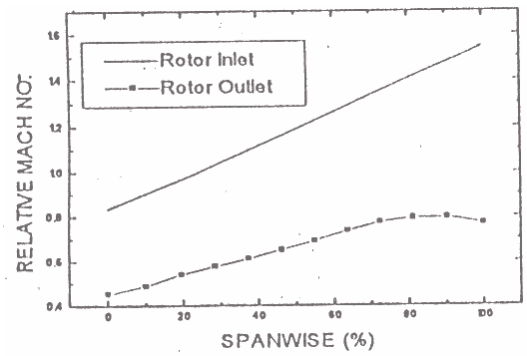

Fig4a:Relative Mach number for rotor at inlet and outlet.

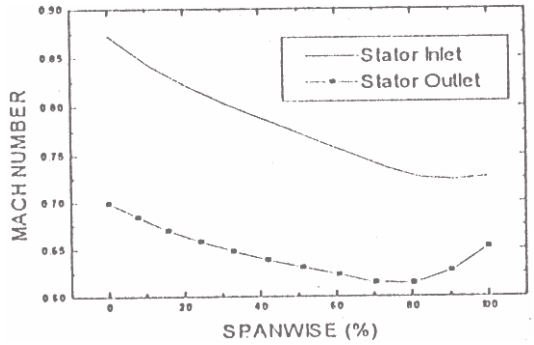

Fig4b: Mach number for stator at inlet and outlet.

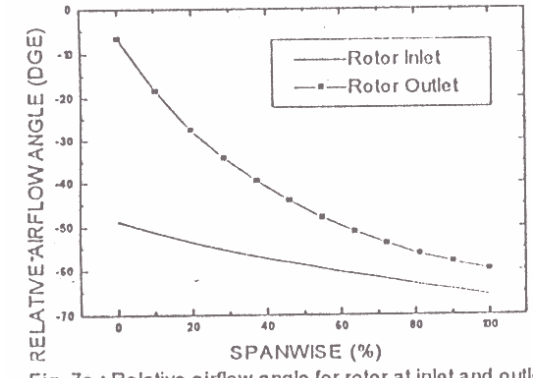

Fig 5a: Relative airflow angle for rotor at inlet and outlet

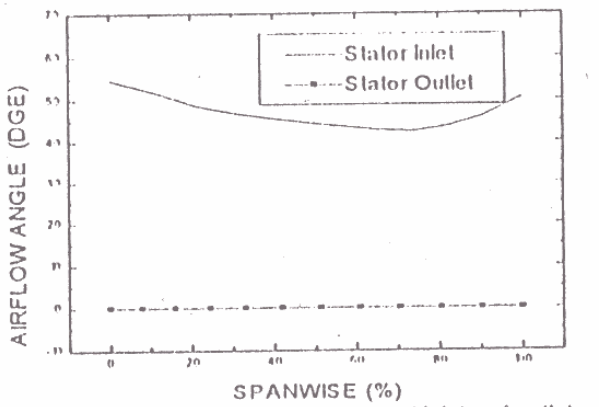

Fig 5b: Relative airflow angle for stator at inlet and outlet

Fig3 to Fig5 show the distributions of pressure ratio, Mach number and air flow angles for rotor and stator at inlet and outlet, respectively.

Blading:

Airfoil camber line:
Rotor: Arbitrary camber line is used for both rotor and stator blades. The distribution of the camber along the chord is determined according to the local loading and inlet Mach number. The position of the maximum

camber is shifted towards the rear part of the chord, from hub to tip in order to reduce the increase of velocity on the forepart of suction surface near the blade tip and decamber the rear part of blade section near the hub. This produces negative camber at tip in the fore part of the camber. The pre-compression airfoil is beneficial for reducing Mach number upstream of the passage shock.

Stator: The design of camber line of stator profile follows the same principle as that of the rotor. The inlet Mach number of stator increases from tip to hub. Hence the front part of hub camber line is decambered. while in the tip region, the camber line approach a circular arc.

Incidence:

The determination of incidence angle was firstly chosen according to the conventional rule, and then modifications were made based on suggestions of 3D calculation result. For example, the incidence of rotor hub is reduced so that the distribution of Mach number along suction and pressure surface shows reasonable loading level at leading edge. The incidence of stator hub is increased as a result of the same consideration.

Deviation:

The deviation of rotor hub is deliberately reduced to a low value in an attempt to eliminate separation, which was detected in 3D calculation.

Stacking:

A complete blade is formed by stacking airfoils along a specified stacking line. A meridional sweep is obtained by specifying an axial displacement distribution of the stacking line referred to a radial line. By the same way, a circumferential lean is obtained by specifying a tangential displacement distribution of the stacking line referred to the same radial line.

As the flow angle varies from hub to tip the case of turbomachine blade row, we will introduce an effective sweep angle instead of a simple definition of sweep angle for plane wings of aircraft. The effective sweep angle γ is defined as

$$\gamma = 90^0 - \theta$$

$$\cos\theta = i_l \cdot i_w$$

Where i_l is the unit vector of the tangent to the locus of blade leading edge points. i_w is the unit vector of relative velocity for rotor.

Fig . 6 shows the effective sweep angle of Q11 rotor blade. We can see from the figure that the effective sweep angle at the tip is as high as 31 degrees, though the meridional sweep is only 18 degrees. The distribution of sweep has further undergone changes in the subsequent configurations based on aerodynamic studies and stress analysis.

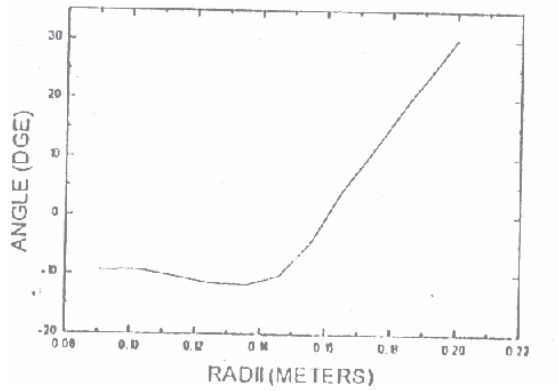

Fig 6: The effective sweep angle distribution of rotor blade

3D computation

Design point

Influence of tip structure on performance:

To clarify the influences of tip structure on performance, computations were made for different tip configurations. Computation indicated that part tip shroud on the back result in higher efficiency. However from the considerations of stress and blade deformation, full shroud was chosen for the rotor.

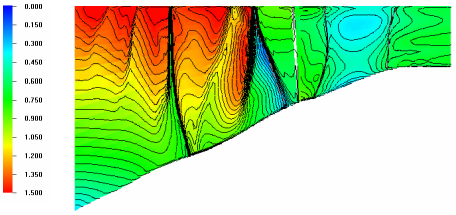

Fig7a:Mach no. contour in meriodional view for suction stream surface.

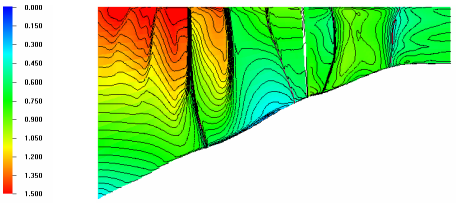

Fig7b:Mach no. contour in meriodional view for pressure stream surface.

Fig7a & Fig7b shows the Mach number contour in meridional view for near suction and pressure streamsurfaces, respectively. The figure shows that the shock wave system of rotor in meridional view leans

back from hub to 70%span then to forward, so there exits a "normal" shock wave section.

Off –design performance

As the 3D code deals with direct (analysis) problem, it allows us to calculate the off-design performance of fan simply by changing the back pressure. On the present report, only performance at design rotation speed is given (Fig7).

The surge margin based on design pressure ratio is:

$$SM\% = \left(\frac{G_d \ \pi^*_s}{G_s \ \pi^*_d} - 1 \right) \% = 11\%$$

Where subscripts d and s stand for design ($\pi^* = 2.135$) and near stall point, respectively.

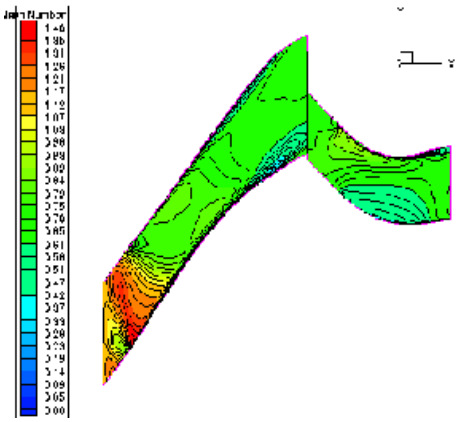

Fig8a: Mach no contour at mid span (near stall)

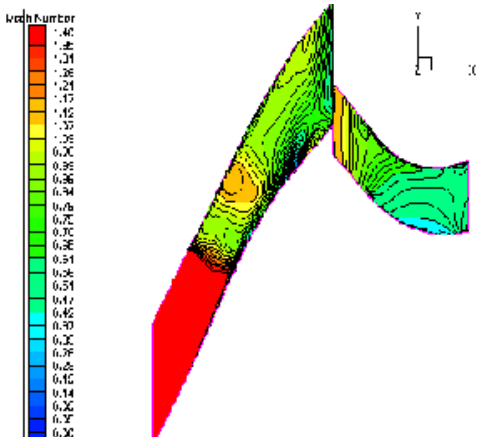

Fig8b: Mach no contour at casing (near stall)

Fig 8a & Fig8b show Mach number contours near stall point for typical stream surfaces at different span wise locations. We see that the shock wave system of mid span section has been pushed out off inlet mouth, while that of tip section still remains inside the mouth. This is a special feature related to forward sweep which will probably improve stall margin.

Some assessments on the 3D computation results:

The result of three-dimensional calculations shows that the design meets the design specifications. According to past experience, this prediction should be obtainable.

The calculated mass flow rate at design point, 20.3 kg/s, is slightly higher than its intended design value, 19.85 kg/s.

As mentioned above, the design value of pressure ratio is 5% higher than its specification. The 3D results suggest that this value maybe slightly higher than needed, because the stall margin based on the design pressure ratio 2.135 is 11.8%, if based on its specification, 2.0, the calculated SNM could reach 20.7%.

If the calculated SM is 5% higher than that really attainable, then a slight reduction of the design pressure ratio is possible.

Further refinement is possible.

Results of 3D computation and Configurations analysed:

Configurations:

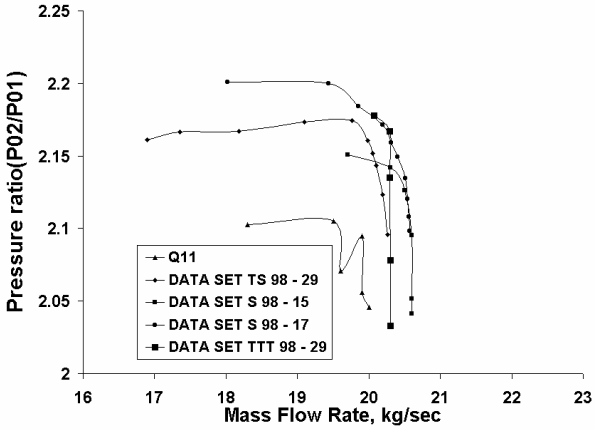

Fig9: Comparison of different configurations.

The fan stage has undergone a series of aerodynamic design improvements (Fig9). The first design configuration Q11[2] was improved to S98-15 [3] based on the study of design configuration worked out by Wadia et al [6]. 3D analysis of Q11 showed the shock swept forward. In the later design this was overcome by lowering the loading level of the tip moving the shock backwards. At the same time Mach number upstream of the shock was controlled by

camber line with precompression. This change in the design resulted in improvement in the fan efficiency by 2%. This design was further modified to S98–17 by increasing the blade tip chord to increase the stall margin [4]. The stress analysis carried out using analysis at NAL indicated high local stress levels in the blades. To limit these stress levels, the blade sections were shifted circumferentially with reference to stacking line. This was further modified to incorporate thick leading and trailing edges as required for CFC blade fabrication. The resulted configuration was TTT 98-29.

Comparison of CFD results

TTT 98-29 was also analysed at NAL using un_b3d_ke (W.N.Dawes). Fig10a-d shows comparison of results of BUAA and NAL for the configurations TS 98-29 and TTT 98-29 isomach number contours in the blade to blade surface indicates stronger shock in NAL results.

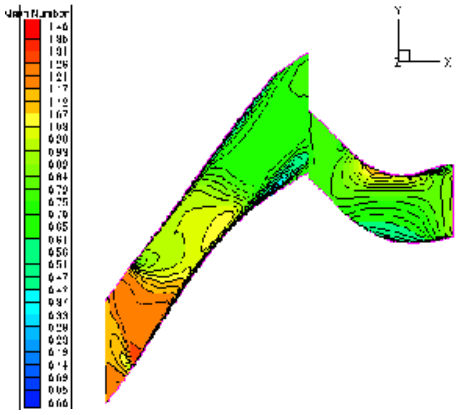

Fig 10a:Mach no contour at mid span (blade to blade) (BAUU)

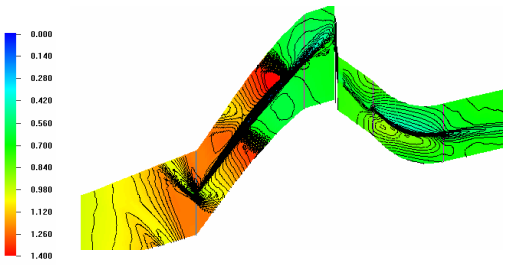

Fig 10b :Mach no contour at mid span (blade to blade) (NAL)

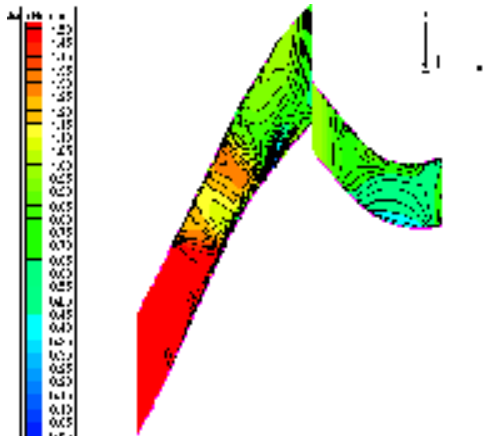

Fig 10c: Mach no contour at casing (blade to blade) (BAUU)

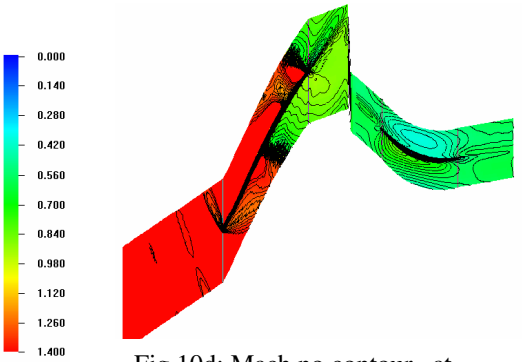

Fig 10d: Mach no contour at casing (blade to blade) (NAL)

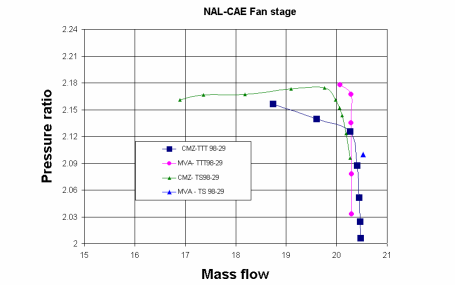

Fig11a: Comparison of fan stage pressure ratio from CFD analysis of BUAA and NAL

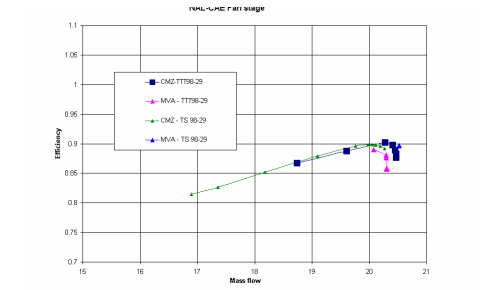

Fig11b: Comparison of fan stage efficiency from CFD analysis of BUAA and NAL

Stress analysis

Advanced composite materials having high strength and low density characteristics such as Carbon/Epoxy looks candidate material for fan stage to exploit aerodynamic advantage of blade configuration having forward sweep and lean. Such blade configurations are expected to experience high stresses due to its complex shape under high rotational speed. Composite materials can be designed to have desired properties without compromising on density.

Fan stage blade

The blade geometry is to be finalised based on aerodynamic performance in conjunction with mechanical integrity of the blade. Finite Element analysis was carried out to evaluate stress and deformation on the proposed fan stage with each blade configuration to assess mechanical integrity. Stress analysis was of preliminary type with much simplification to obtain reasonably good results. In order to bring down the stress level in the final stages of stress analysis, the blade sections were shifted circumferentially with reference to stacking line. This is further modified to incorporate thick leading and trailing edges as required for Carbon Fiber Composite (CFC) blade fabrication. The resulted configuration is "TTT98-29". Stress analysis carried out on this blade is briefly presented as below.

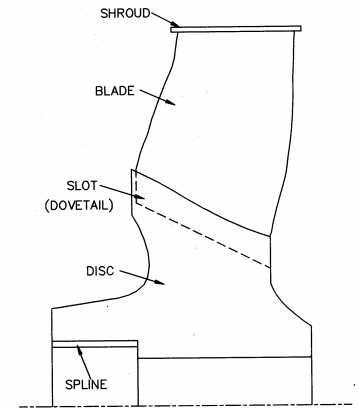

Fig 12: FANSTAGE BLADE WITH DISC

The fan stage blade is scaled down to 79% to match the available drive motor power. The blade tip radius of full scale model 200mm becomes 158 mm after scaling. The blade root radius is 71mm at the leading edge and smoothly increases to 99mm at the trailing edge. The blade thickness at the mid chord of the root and tip are about 5.5 and 2.1 mm respectively and taper off to zero value at the edges on either side. Suitable hub and shroud are to be added as part of the analysis. A constant thickness 2.25mm is chosen for the shroud. The blade has dovetail root and is inserted into the slot of the disk. The schematic of bladed disk with shroud is shown in figure-12. The hub is extended so that it can be attached to drive shaft with spline. The fan stage rotates at 28,400 rpm to keep 470m/s tip speed.

Finite element analysis

The blade is viable only with the use of CFC as material with its unique property of low density to high strength ratio. The complex aerodynamic shape of the blade with forward sweep and lean, variation in thickness and large amount of twist makes modeling an intricate task and is expected to produce very high stress spots. Use of carbon composite whose properties are highly direction oriented involves additional complexity. Therefore, Finite Element technique comes out as the only tool for the stress analysis.

Stress analysis of this fan stage was carried out using MSC/NASTRAN. Stress and deformations were predicted under the combined loads of inertia force for the steady state operation of the fan stage at 28,400rpm and static pressure. Since the inertia load changes with deformation of the blade, stress analysis was carried out with geometric non-linear analysis option.

Finite element model

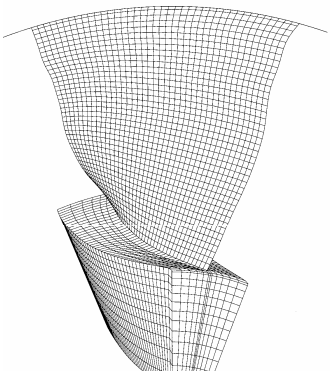

Fig 13: Finite Element Model of Compressor Sector model with Hub, Blade and Shroud (Blade Mesh: 40x40, Axial x Spanwise)

A sector model was employed taking advantage of cyclic symmetry of the bladed disk. There are 17 blades and a disk sector (hub and shroud), which subtends 360/17 degrees at the center along with a whole blade, is isolated. The sector surfaces are parallel to the blade camber line and are at mid plane in between adjacent blades.

The hub in the sector model was meshed to have 8 noded hexahedron or brick elements. The blade and the shroud were to be fabricated using layered composite and are modeled using the shell (4 noded quadrilateral) element. The finite element of the sector is shown in figure-13. A layer thickness of 0.15mm is chosen and the number of layers in each element was obtained based on centroidal thickness of the shell element. The blades have dovetail root and are inserted into the slots made in the disk. However in the finite element model, Rigid links were used to attach the blade shell elements with the hexahedral elements of the full solid hub. The fiber orientation in the layers follows a regular repeating order about the middle layer as given below with as many layers as required to match the thickness. The centroidal thickness of each element was obtained from the aerodynamically designed blade configuration. A few more layers were added to the elements along the blade root as well as to elements along the blade tip in addition to the layers which were arrived at based on aerodynamic shape of the blade to account for the fillet. Fabrication of fan stage with composite introduces a large fillet both at the hub & blade root and blade tip & shroud interface regions. The layers added corresponds to a ranges of thickness from 0.3 to 0.9mm to approximately simulate the fillet.

The number of layer ranges from a mere 3 at the blade edges to a maximum of 51 at the blade root. Zero degree fiber orientation in the blade aligns with radial direction. In the case of shroud, the zero degree fiber orientation means circumferential direction.

Lamination sequence (Fiber Orientation Angle, degrees):

...0/0/-45/45/0/0/-45/45/0/45/-45/0/0/45/-45/0/0…
1
middle layer

Material properties of Carbon/Epoxy composite used for blade and shroud are presented in Table -1.

Table-1 Lamina Properties used for Carbon/Epoxy

Axial Stiffness	=	131.0 GPa
Transverse Stiffness	=	10.1 GPa
Shear Stiffness	=	3.6 GPa
Poisson's Ratio	=	0.3
Specific Gravity	=	1.7

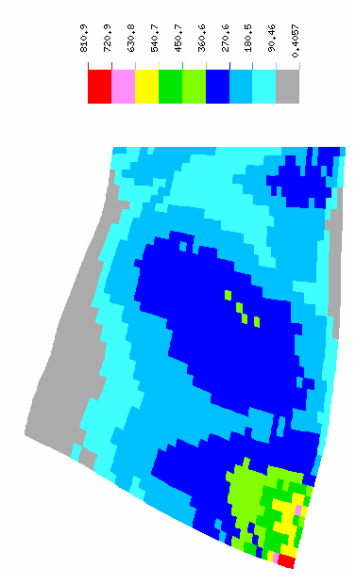

Fig 14a : Maximum Tensile Stress along the fiber direction(Sxx) (maximum stress in a layer in each element)

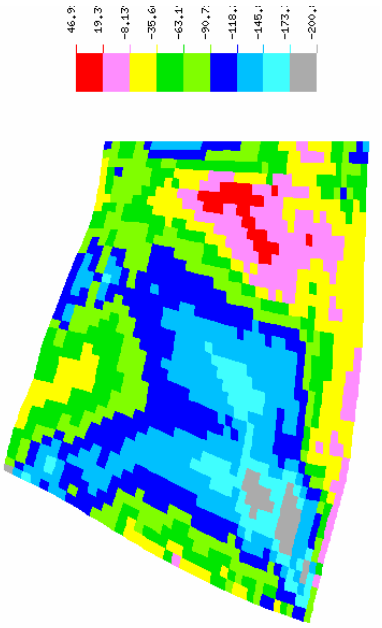

Fig 14b : Maximum Compressive Stress along the fiber direction(Sxx) (maximum stress in a layer in each element)

Stress analysis results

Deformation and stress results are obtained for the model using non-linear geometry option under the combined inertia and pressure loads. The maximum blade deformations are 0.40, 0.56 and 1.27 mm in the radial, circumferential and axial direction respectively. The deformation and stress plots of blade are presented

on blade projected on the meridional plane with hub and shroud removed for the sake of clarity.

The stress along the fiber direction (longitudinal fiber stress-Sxx) in a layer in each element is presented.

These are element stresses, which are constant within the element. Number of layers in the element vary from mere 3 at the leading and trailing edges to 51 at the mid chord of the blade root in proportion to the thickness. Therefore, out of voluminous results, only the stress along the fiber direction in each layer of every element are sampled and the maximum stresses in tensile and compressive nature are presented respectively for the blade in figure 14(a) and 14(b). The maximum tensile fiber stress is 810 M Pa and is found at the leading edge of the blade root. The maximum fiber stress in compression 200 M Pa is found to occur at the blade root tailing edge of the blade. Though these stresses are within the ultimate strength of the CFC , they are in general on the higher side. The presence of shroud is not helping to reduce the blade stresses and deformations.

Concluding Remarks

2D and 3D computations over the fan flow field show that for the defined geometry the required specifications of the fan can be met. The high pressure ratio fan was designed with special features of forward sweep of the blades and reverse camber at the rotor tip for precompression. Design configuration was optimised through 3D viscous analysis for the fan stage performance and stress analysis of CFC rotor blade for strength limits. Performance analysis of the fan stage carried out both at BUAA and NAL indicate good matching of rotor and stator at high Mach number condtions.

Acknowedgements

Authors are thankful to Chinese Aeronautical Establishment, China and National Aerospace Laboratories, Bangalore for supporting this joint project..Authors thank Mr. Q.H.Nagpurwalla and Mr.S.A.Guruprasad who are responsible for development and testing of the fan stage at NAL for their coordination and necessary inputs.

References

[1] A.R. Wadia, P.N. Szucs, D.W. Crall: “Inner working of aerodynamic sweep”, ASME Paper No. 97-GT-401, 1997.

[2] M.Z. Chen, H.K. Jiang, Peng Bo, Xu Liping: “Aerodynamic Design Report of a single stage fan with 2.0 pressure ratio”, BUAA Report, 1996.

[3] M.Z. Chen, H.K. Jiang, Peng Bo, Xu Liping: “Report on further investigation of aerodynamic design of a single stage fan with pressure ratio 2.0”, BUAA Report, 1998.

[4] M.Z. Chen, H.K. Jiang, Xu Liping: “Aerodynamic design of S98-17 and S98-18”, BUAA Report, 1998.

[5] M.Z. Chen, H.K. Jiang, Xu Liping: “Aerodynamic design of S98-29”, BUAA Report, 1998.

[6] Q.H. Nagpurwala, M.V.A. Murthy, S.A. Guruprasad, M. Jayaraman, Gangan Prathap, R.M.V.G.K. Rao, L.R. Chandramohan, B.R. Pai: “A report on the progress of work and the current status of the NAL-CAE joint programme on design, development and testing of a high pressure ratio axial fan stage”, NAL PD PR 9812, 1998

[7] M.Jayaraman, M. Subba Rao, Gangan Prathap, ‘ Stress Analysis of a Carbon/Epoxy Composite High Pressure Ratio Axial fan Stage’, [Blade Configuration: Q11], PD PR 9803, April 1998, National Aerospace Laboratories, Bangalore- 560 017, India.